Electrochemical capture and conversion of CO_2 into syngas

Yongwook Kim,[1#] Eric W. Lees,[2#] Chaitanya Donde,[2] Christopher E.B. Waizenegger,[1] Grace L. Simpson,[1] Akshi Valji,[2] and Curtis P. Berlinguette*[1,2,3,4]

[1]Department of Chemistry, The University of British Columbia, 2036 Main Mall, Vancouver, British Columbia, V6T 1Z1, Canada.

[2]Department of Chemical and Biological Engineering, The University of British Columbia, 2360 East Mall, Vancouver, British Columbia, V6T 1Z3, Canada.

[3]Stewart Blusson Quantum Matter Institute, The University of British Columbia, 2355 East Mall, Vancouver, British Columbia, V6T 1Z4, Canada.

[4]Canadian Institute for Advanced Research (CIFAR), 661 University Avenue, Toronto, M5G 1M1, Ontario, Canada.

[#]These authors contributed equally to this work

*Correspondence: Curtis P. Berlinguette (cberling@chem.ubc.ca)

Abstract

For waste CO_2 to be electrolytically converted into higher-value chemicals and fuels, electrolyzers that drive the CO_2 reduction reaction need to be integrated with upstream CO_2 capture units. However, this has not yet been demonstrated because of the large operational gap for the capture and conversion steps. Here, we report a coupled carbon reactor that captures and converts CO_2 into syngas with a 1.7:1 ratio of H_2 to CO. The resulting syngas can be utilized in the production of a wide range of valuable chemicals. This CCR uses a packed bed absorption column ("capture unit") to react alkaline aqueous solution enriched in $K_2CO_{3(aq)}$ with CO_2 to form bicarbonate enriched solutions ("reactive carbon solutions"). These reactive carbon solutions are then fed into an electrochemical reactor ("bicarbonate electrolyzer") to form $CO_{(g)}$ and OH^- product. This alkaline product is then passed through a gas-liquid separator ("separator") and recycled back to the capture unit for further reaction with $CO_{2(g)}$. These collective elements close the full loop for CO_2 capture and conversion. An electrochemically inert CO_2 capture promoter (glycine) was used to better match the CO_2 capture rates in the absorption column to the OH^- production rates in the electrolyzer, thereby producing CO at steady-state without intervention. We demonstrate that the CCR captures and converts CO_2 from simulated flue gas (20% CO_2; 80% N_2) into CO with a Faradaic efficiency of 30% at 100 mA cm^{-2} for 30 hours of operation.

Introduction

The electrolytic reduction of CO_2 into higher value products offers the opportunity to offset the high cost of carbon capture by generating a new revenue stream from waste CO_2. One possible pathway for achieving this goal would be to combine the direct air capture approach developed by Keith et al.,[1] with an electrolyzer capable of converting $CO_{2(g)}$ into product (e.g., CO). This pathway for the capture and utilization of CO_2 would involve four steps presented in Fig. 1: (i) reaction of CO_2 with alkaline solution to form an aqueous "reactive carbon solution" enriched with (bi)carbonates;[1] (ii) desorption of CO_2 from the reactive carbon solution to regenerate the CO_2-lean form of the sorbent; (iii) pressurization of the purified CO_2; and (iv) electrochemical upgrading of the CO_2 gas into CO product in an electrolyzer. The CO_2 capture, desorption, and pressurization units are capital intensive, and therefore require continuous operation at the megatonne scale to justify the upfront investment.[2] The electrochemical reactor is modular and can ramp production up or down in response to electricity surpluses.[3,4] These tradeoffs in terms of scale and operation will increase the capital and operating cost of the CO_2 capture and conversion units at scale. Consequently, CO_2 capture units have not yet been coupled to a CO_2 reduction reaction (CO2RR) electrolyzer for continuous, closed-loop operation at scale.

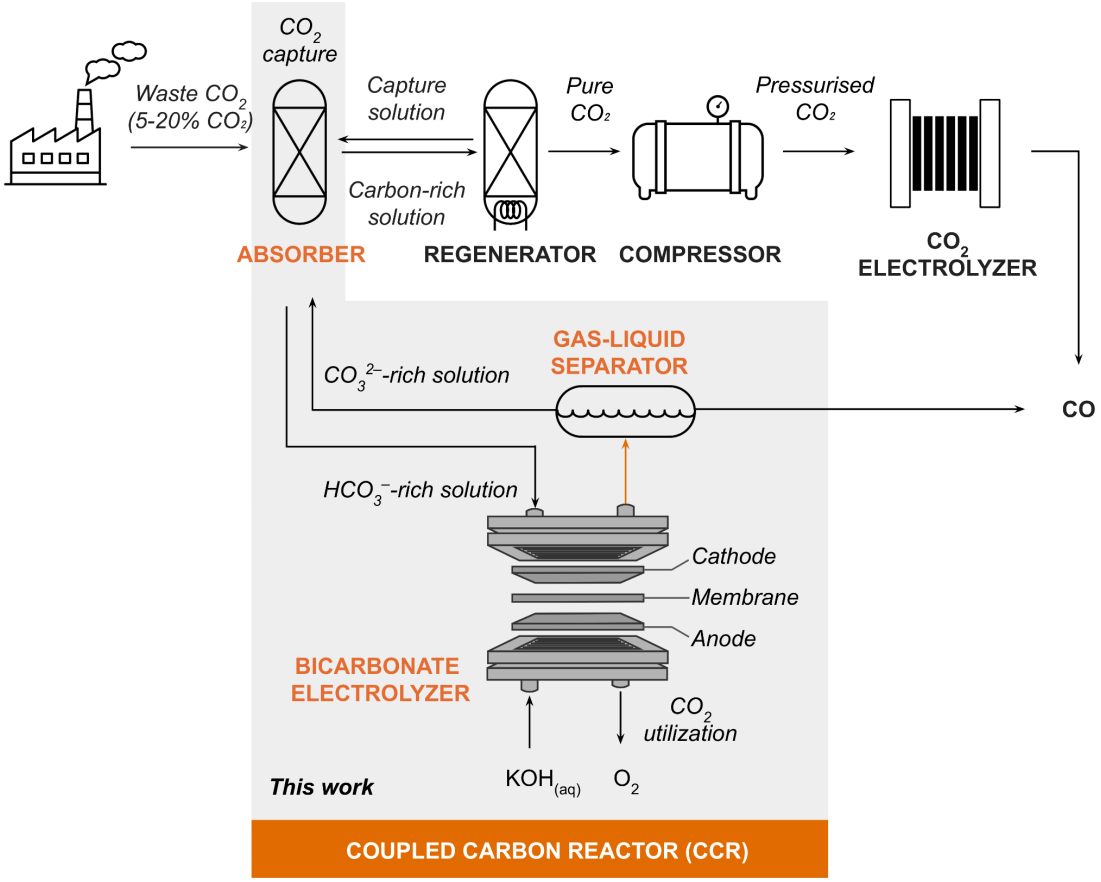

Fig. 1. A schematic representation of two distinct electrochemical pathways for CO_2 capture and utilization. In both pathways, an aqueous sorbent reacts with CO_2 to form a "reactive carbon solution" that is enriched with (bi)carbonate ions. The black pathway captures and converts CO_2 independently and consequently requires an energy-intensive CO_2 recovery step to generate a pure CO_2 stream for the CO_2 electrolyzer. The orange pathway, known as the bicarbonate electrolyzer pathway, enables the bypass of this energy-intensive step, resulting in a higher energy efficiency.

To address this challenge, we designed a class of electrochemical reactors that electrochemically convert reactive carbon solutions (rather than pressurized CO_2 feedstocks) into CO2RR products in a single step (Fig. 1; "bicarbonate electrolyzer").[5–8] These "bicarbonate electrolyzers" mediate reactive carbon capture by electrochemically generating H^+ to convert (bi)carbonates into CO_2 *in situ* (denoted herein as "*i*-CO_2"). This formation of *i*-CO_2 (Eq. 1) at the cathode|membrane interface enables bicarbonate electrolyzers to achieve higher process energy efficiencies than gas-fed CO2RR electrolyzers by eliminating the energy penalty (>100 kJ mol^{-1}) associated with generating a pure stream of CO_2 gas.[8–11] This *i*-CO_2 is subsequently reduced at the surface of an electrocatalyst to produce

carbon-containing compounds and OH^- (Eq. 2). The OH^- can be recycled to capture additional CO_2 (Eq. 3).

$$HCO_3^-{}_{(aq)} + H^+{}_{(aq)} \rightleftharpoons CO_{2(g)} + H_2O_{(l)} \quad (1)$$

$$CO_{2(g)} + H_2O_{(l)} + 2e^- \rightarrow CO_{(g)} + 2OH^-{}_{(aq)} \quad (2)$$

$$CO_{2(g)} + OH^-{}_{(aq)} \rightleftharpoons HCO_3^-{}_{(aq)} \quad (3)$$

All bicarbonate electrolyzers reported to date were fed with laboratory-prepared solutions saturated with bicarbonate ions (because CO_2 reacts with OH^- to form HCO_3^-; Eq. 3). However, these solutions do not match the effluent from practical CO_2 capture units, such as a CO_2 absorption column.[12–17] It is therefore unknown if the OH^- produced during CO2RR (Eq. 2) within a bicarbonate electrolyzer regenerates sufficient alkalinity to enable continuous CO_2 capture at steady-state. We therefore set out to couple a carbon capture unit with a bicarbonate electrolyzer to form a "coupled carbon reactor" (CCR; Fig. 2), and to test the continuous operation of the CCR.[18]

Here, we built a laboratory-scale CCR with a packed-bed CO_2 absorption column, a bicarbonate electrolyzer, and a gas-liquid separator to continuously capture and convert CO_2 from simulated flue gas (20% CO_2; 80% N_2) into CO. We used an aqueous K_2CO_3 sorbent, which is used at a large scale through the Benfield process,[19] containing promoters such as glycine. These promoters enabled modulation of the dynamic rates of CO_2 capture and CO formation in the absorption column and bicarbonate electrolyzer, respectively. We report here a set of experimental conditions where the CCR yields FE_{CO} of 30% at 100 mA cm^{-2} for 30 hr without intervention or any significant decline in performance. To our knowledge, this report is the first example of a closed-loop system capable of capturing and converting CO_2 into a higher value product.

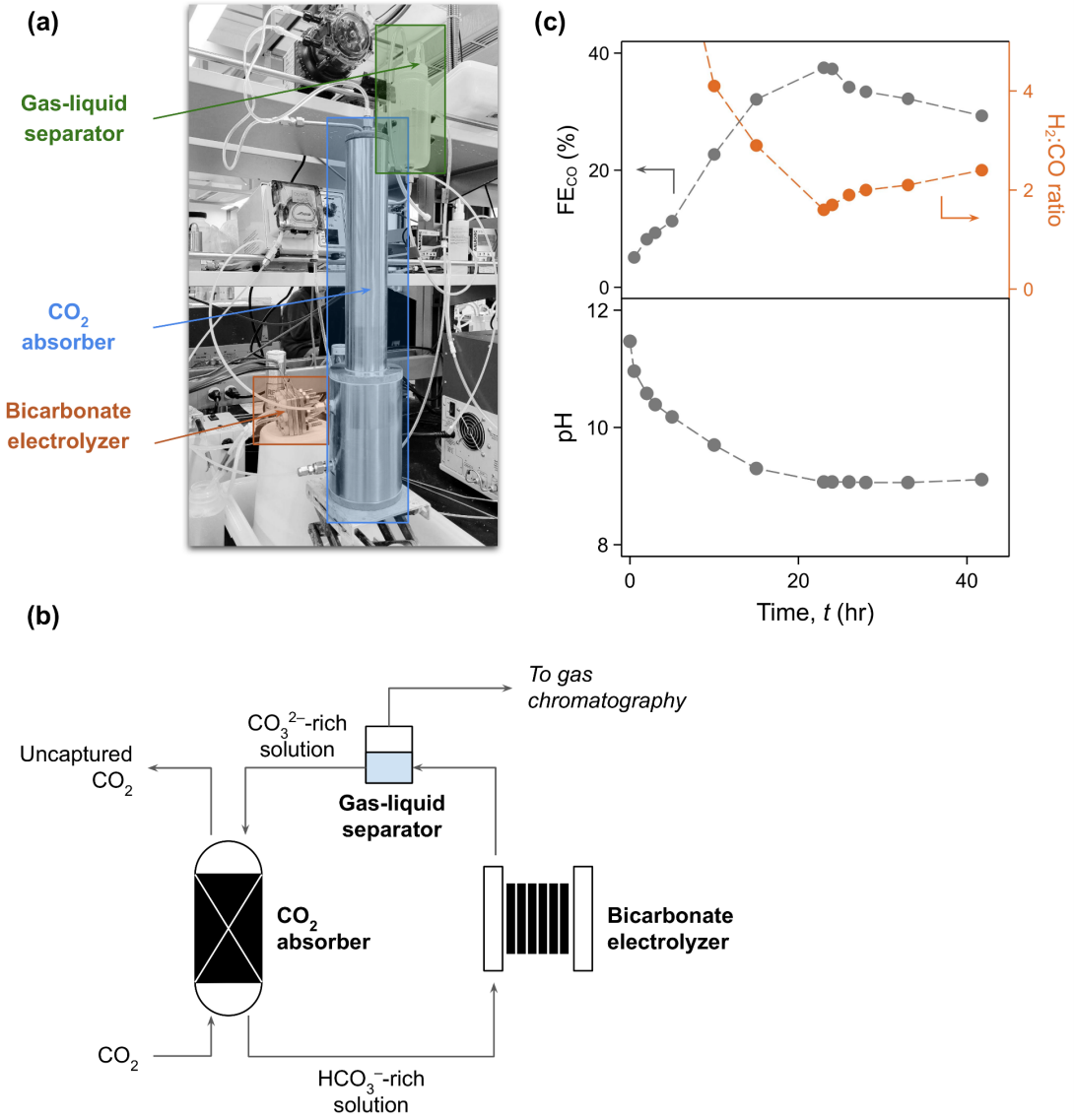

Fig. 2. The coupled carbon reactor (CCR) for integrated CO_2 capture and utilization. Data shown in this figure were obtained using an unpromoted 1 M K_2CO_3 reactive carbon solution. (a) Photograph of the CCR setup, including the absorption column, bicarbonate electrolyzer, and gas-liquid separator. (b) Schematic representation of the CCR and the streams entering and leaving each unit. (c) Steady-state CO formation during sustained electrolysis at 100 mA cm^{-2} and measured pH of the reactive carbon solution exiting the bicarbonate electrolyzer as a function of time. The CCR produces a syngas ratio (H_2:CO) of 1.7.

Results

Capture Unit. We designed and built a CO_2 absorption column to resemble an industrial CO_2 capture unit. The CO_2 absorption column consisted of a stainless steel vessel (diameter: 4 cm; height: 30 cm) filled with a 20-cm tall packed bed of polypropylene Raschig rings (length: 0.8 cm; outer diameter: 0.6 cm; and inner diameter: 0.4 cm). The CO_2 absorption column was designed to operate in a counter-current mode, where the flow of simulated flue gas that entered at the bottom of the packed bed opposed the flow of liquid reactive carbon solution that entered at the top of the column (Fig. S1; also see Methods and Materials in Supplementary Materials).

To establish a baseline for carbon capture performance, we compared the CO_2 capture rate in the CO_2 absorption column to that of a single-state sparging apparatus (i.e., a "CO_2 bubbler"; Fig. S2) using unpromoted 1.5 M K_2CO_3 solutions as the sorbent. We supplied 100 sccm of 50% CO_2 (balance N_2) for both apparati. When operated independently of the CCR, the CO_2 absorption column enabled a 10-fold increase in CO_2 capture rates compared to the CO_2 bubbler, evidenced by a drop in pH from 12 to 10 in 1 hr (Fig. S2; Tables S1 and S2; see Supplementary Note 1 for calculations).

Bicarbonate electrolyzer. We built a bicarbonate electrolyzer consisting of stainless steel housing plates and flow plates with serpentine patterns that sandwiched the nickel foam anode, bipolar membrane, and the silver cathode spray-coated on carbon paper (Fig. 1). The membrane and electrodes were firmly pressed against each other with no gap ("zero-gap architecture"). The active area of the bicarbonate electrolyzer was 4 cm^2.

Coupled carbon reactor ("CCR"). The CCR was assembled by integrating a CO_2 absorption column ("absorber"), a bicarbonate electrolyzer, and a gas-liquid separator ("separator") (Fig. 2). The separator, which was designed as a sealed reservoir, functioned to separate the gaseous products (CO and H_2) from the reactive carbon solution. The liquid outlet of the absorber was linked to the inlet of the bicarbonate

electrolyzer, while the outlet of the bicarbonate electrolyzer was connected to the inlet of the separator. Finally, the outlet of the separator was connected to the inlet of the absorber, thus establishing a closed loop of liquid flow.

CCR Proof-of-Concept Experiment. We then performed a CCR experiment with a 1 M K_2CO_3 reactive carbon solution. This proof-of-concept CCR experiment was initiated by feeding 1000 sccm of simulated flue gas (20% CO_2; 80% N_2 by volume) to the absorber, applying a constant current density of 100 mA cm^{-2} to the electrolyzer, and circulating the CO_2-lean form of the 1 M K_2CO_3 reactive carbon solution through the three CCR components (absorber, electrolyzer, and separator). Gas chromatography (GC) analysis was used to analyze the composition of the gas stream exiting the top of the separator. Further details on experimental setup and procedure are found in the Methods and Materials section of the Supplementary Materials.

We observed an increase in FE_{CO} from 5% to 37% in the bicarbonate electrolyzer over the first 23 hours of CCR operation using unpromoted 1 M K_2CO_3 (Fig. 2). This FE_{CO} value of 37% corresponds to a H_2:CO ratio of 1.7:1, which is relevant to diesel synthesis.[20] The FE_{CO} then progressively declined to 29% over the next 20 hours of operation. A decrease in pH of the reactive carbon solution tracked the increase in FE_{CO} until a steady-state pH of 9.1 was reached (Fig. 2). This steady-state pH of the solution corresponds to a CO_2 loading of 0.88 mol CO_2/mol K^+.[21,22] These collective results are all consistent with expected (bi)carbonate equilibria and acid-base kinetics associated with CO_2 capture and electrochemical CO_2 desorption.[5]

Promoters help match rates of CO_2 capture and conversion.

We first performed a series of experiments independently in a bicarbonate electrolyzer and measured the FE_{CO} (Fig. S3). A nickel foam anode, bipolar membrane, and silver spray-coated carbon paper cathode comprised the membrane electrode assembly. A 1 M KOH solution was fed to the anode

compartment and a 3 M $KHCO_3$ solution, containing either 0.1 M piperazine or 0.1 M glycine, were delivered to the cathode compartment. The electrolysis experiment with an unpromoted 3 M $KHCO_3$ solution yielded FE_{CO} of 75%. When a 3 M $KHCO_3$ solution doped with 0.1-M piperazine was used as the catholyte, the FE_{CO} substantially decreased to 13%. The 3 M $KHCO_3$ solution doped with 0.1-M glycine yielded a FE_{CO} of 56%.

Next, we quantified the impact of CO_2 capture promoters on CCR operation. We performed CCR experiments with 1 M K_2CO_3 solutions doped with 0.1 M piperazine and 0.1 M glycine and monitored the CO_2 capture rate in the absorber (i.e., pH change) and FE_{CO} of the bicarbonate electrolyzer (Fig. 3). All experiments were performed in triplicate. When 1 M K_2CO_3 solution was doped with capture promoters, the steady-state pH decreased from 9.1 for unpromoted to 8.9 for both promoted solutions. We observed a 4- and 2-fold increase in CO_2 capture rates with the piperazine- and glycine-doped solutions, respectively, compared to the unpromoted 1 M K_2CO_3 solution (Fig. 3 and Fig. S4). However, the bicarbonate electrolyzer yielded a lower FE_{CO} (5% ± 1%) when the CCR was operated with a piperazine-doped solution compared to an unpromoted 1 M K_2CO_3 solution (FE_{CO} = 35% ± 2%). The glycine-doped solution yielded a similar FE_{CO} as the unpromoted 1 M K_2CO_3 solution (FE_{CO} = 30% ± 3%). These results are consistent with our independent study using a bicarbonate electrolyzer (Fig. S3). The rate of *i*-CO_2 generation at steady state increased when rate promoters were added to the capture solution (Fig. 3). We observed that the addition of glycine enhanced the *i*-CO_2 generation to a higher degree. These results collectively teach that glycine is a more effective promoter for the CCR than piperazine for our experimental conditions.

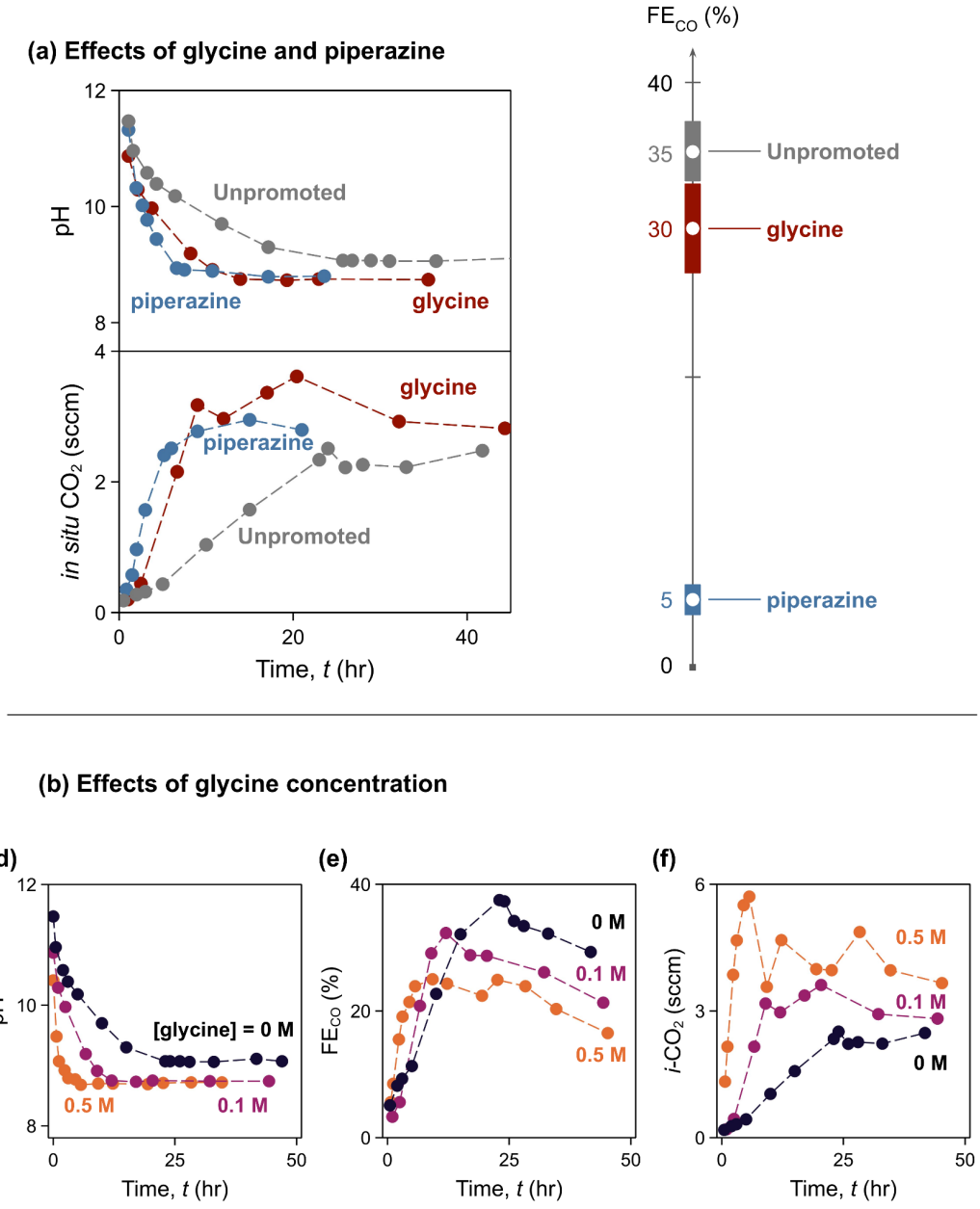

Fig. 3. How promoters affect the operation of the coupled carbon reactor. (a) shows the measured pH, Faradaic efficiencies for CO (FE_{CO}), and rates of *in situ* CO_2 generation (*i*-CO_2) of CCR operated with either piperazine- or glycine-doped reactive carbon solution. Addition of capture promoters increase *i*-CO_2. However, the addition of piperazine to the reactive carbon solution substantially decreases FE_{CO}. (b) shows the effect of glycine concentration (0, 0.1, 0.5 M) in the operation of the CCR (e.g., pH, FE_{CO}, and *i*-CO_2). Increase in glycine concentration increases *i*-CO_2, but decreases FE_{CO}.

With confirmation that glycine is a favorable CO_2 capture promoter for the CCR, we tested the possibility of increasing the glycine concentration to further improve the capture rate in the CCR. We

doped 1 M K_2CO_3 solutions with 0 (control), 0.1 and 0.5 M glycine. All other operating conditions of the CCR (i.e., current density, liquid and gas flow rates) were held at parity with the previous CCR experiments. We observed an increase in CO_2 capture rate with increasing glycine concentrations (Fig. S5). We observed 2-fold and 2.5-fold faster decreases in pH when using 0.1 and 0.5 M glycine, respectively (compared to the unpromoted 1 M K_2CO_3 solution; Fig. 3). However, the steady-state FE_{CO} decreased as the concentration of glycine increased with and without the promoters (Fig. 3).

The concentration of glycine added to 1 M K_2CO_3 also had an impact on the *i*-CO_2. When the concentration of glycine in 1 M K_2CO_3 was increased from 0 M to 0.5 M, the bicarbonate electrolyzer liberated higher amounts of *i*-CO_2 (Fig. 3). This result indicates that glycine, a CO_2 capture promoter, not only helps increase the CO_2 capture rate, but also enables faster electrochemical recovery of CO_2 from a bicarbonate electrolyzer.

Discussion

Amine-based sorbents such as monoethanolamine ("amines") are the most widely used CO_2 capture sorbent in industry. However, aqueous K_2CO_3 solutions can also be used as sorbent, and offer lower regeneration energies, less corrosion, higher durability, and the capture of other impurities such as SO_x and NO_x in the flue gas stream.[23,24] The notion of capturing CO_2 with K_2CO_3 solutions has gained traction since the development of the "Benfield process",[19] but laboratory and pilot scale studies have focused on the design of CO_2 capture units at a large scale (kg hr^{-1} and ton hr^{-1} for laboratory- and pilot-scale studies).[22] A high-performance bicarbonate electrolyzer generates *i*-CO_2 at a rate of g hr^{-1} (e.g., 0.53 g hr^{-1} for a bicarbonate electrolyzer with a 4-cm^2 geometric active area; FE_{CO}: 80%; carbon utilization efficiency: 50%; applied current density of 100 mA cm^{-2}).[7]

The scales of operation for capture (kg to ton hr^{-1} of CO_2 captured) and conversion (g hr^{-1} of CO_2 utilized) are simply not aligned. Consequently, CO_2 capture has not yet been coupled to CO_2 conversion. There are also no reports of CO_2 capture with aqueous K_2CO_3 solutions at smaller scales (g hr^{-1}).

The rate of CO_2 capture and conversion in the CCR is governed by the pH during operation, and by the kinetics of the (bi)carbonate equilibrium (Fig. S6 and Supplementary Note 1).[25] At a high pH regime where CO_3^{2-} ions are the dominant species, the CO_2 capture rate is high but the electrolyzer performance is lower.[5,25] At lower pH values (i.e., pH 8-9), CO_2 capture rate is low but electrolyzer performance is higher (e.g., higher FE_{CO}; Fig. 4). This indirect correlation creates a tradeoff for CO_2 capture and conversion.

A saturated 3 M $KHCO_3$ solution (pH 8.3; see Supplementary Note 3) is effective for electrolysis but too acidic for efficient CO_2 capture. A 1 M K_2CO_3 solution (pH 12) in the CCR is initially effective at CO_2 capture in the column (2.9 g hr^{-1}), but the capture rate progressively decreases to 0.30 g hr^{-1} as the 1 M K_2CO_3 solution absorbs CO_2 and becomes less alkaline Fig. 4). The electrolyzer FE_{CO} increases from 5% to 37% as the pH decreases from 11.5 to 9.1. The pH and FE_{CO} values reach a steady-state when the rate of CO_2 capture in the column (0.30 g hr^{-1}) matches the rate of CO_2 desorption in the

electrolyzer at 0.30 g hr^{-1}. These results are consistent with our previous works, which showed that HCO_3^--rich solutions enable higher CO formation rates than CO_3^{2-}-rich solutions.

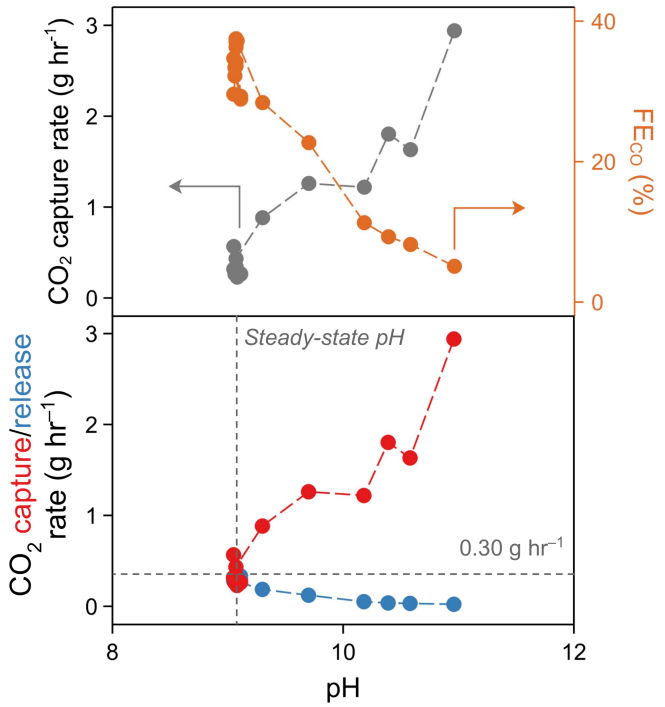

Fig. 4. Tradeoff between the performance of the CO_2 absorption column and the bicarbonate electrolyzer. The top panel shows the effect of pH on CO_2 capture and CO formation: at high pH, CO_2 capture is favored while CO formation is reduced, whereas at lower pH (~8-9), CO formation is enhanced but CO_2 capture is limited. The bottom panel depicts the interplay between the rates of CO_2 capture in the absorption column and CO_2 desorption from the bicarbonate electrolyzer, which generates CO_2 *in situ*. The pH of the system reaches a steady state when these two rates are balanced.

For both promoted and unpromoted (bi)carbonate solutions, we observed a gradual decrease in FE_{CO} over time after the peak value was reached (Figs. 2 and 5). However, the steady-state pH and *i*-CO_2 formation rates remained approximately constant throughout the entire experiment (~40 h), indicating that the solution chemistry enabling synchronized CO_2 capture and *i*-CO_2 formation was preserved. We therefore hypothesized that mass transport limitations caused by the accumulation of bubbles in the cathode chamber of the electrolyzer were causing the FE_{CO} of the CCR to decrease over time. To test this hypothesis, we performed an experiment where the flow rate of 1 M K_2CO_3 through the CCR was pulsed

from 100 mL min^{-1} to 150 mL min^{-1} for 30 sec when the FE_{CO} was observed to decline from its peak value of 37% to 29% (i.e., after 40 h of operation at 100 mA cm^{-2}; Fig. 5). During the pulse, we observed a brief 20-mV drop in cell potential (Fig. S7), which is consistent with a reduction in bubble-induced Ohmic resistances in the cathode.[26] Moreover, the FE_{CO} measured 1 hr after the flow rate pulse showed a complete recovery to 37%. The FE_{CO} decreased again to 30% during the next 3 hr of electrolysis, but the peak FE_{CO} value of 37% was recovered once again by repeating the pulsing protocol after 43 hr of electrolysis.

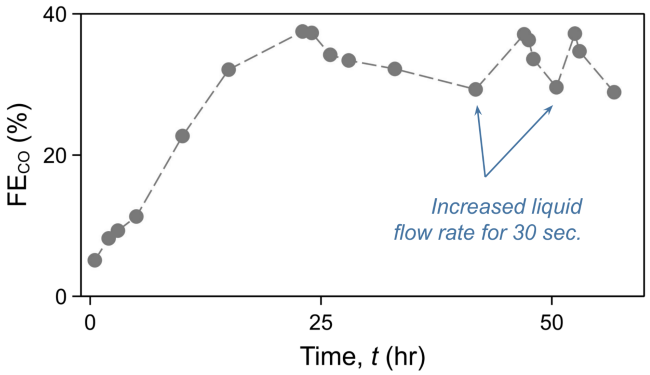

Fig. 5. **The importance of bubble management in the extended CCR operation.** The impact of periodically increasing the liquid flow rate on the Faradaic efficiencies for CO formation (FE_{CO}) during electrolysis with the unpromoted CCR. A gradual decrease in the FE_{CO} is observed after 1 day of CCR operation. However, this decrease in FE_{CO} is completely recovered when the liquid flow rate is increased from 100 mL min^{-1} to 150 mL min^{-1} for 30 sec.

A drawback of using K_2CO_3 as a sorbent is the slow reaction kinetics between CO_2 and OH^- (Eq. 3). This slow reaction necessitates a tall CO_2 absorption column to achieve a high absorption efficiency, which equates to higher capital and operating costs. To address this issue, chemical compounds can be added to the sorbent to accelerate the rate of reaction between CO_2 and the sorbent. Piperazine[27] and glycine[28,29] are known to enhance by >500% the reaction kinetics between CO_2 and alkaline sorbents, but the impact of these rate promoters on reactive carbon capture is not known. If the carbonate-based CCR were to be commercialized, these rate promoters will likely need to be implemented into the CCR to

reduce investment costs.

We therefore incorporated these rate promoters into the CCR to achieve higher rates of CO_2 capture at lower pH values. The addition of 0.1 M and 0.5 M glycine to the CCR increased the rate of electrochemical CO_2 capture and desorption from 0.27 to 0.35 and 0.42 g hr^{-1}, respectively. These additions of glycine exhibited nominal effects on FE_{CO} (Fig. 3 and Fig. S5). In stark contrast, the addition of piperazine to the CCR dramatically decreased the FE_{CO}, which we attribute to differences in the rate of (bi)carbonate and carbamate formation for the two promoters.[30–34]

The capture promotion mechanism for both glycine and piperazine proceeds through two steps: (i) the formation of a zwitterionic carbamate intermediate (denoted $R_1R_2NH^+COO^-_{(aq)}$; Eq. 4); and (ii) the deprotonation of the intermediate by a base (denoted **B**; Eq. 5) such as H_2O, OH^-, HCO_3^-, CO_3^{2-}, or another zwitterionic carbamate (Eq. 6).[35] For the system promoted with glycine, the deprotonation of zwitterionic carbamate is faster than the zwitterionic carbamate formation due to the ionic charge associated with glycine.[34,36,37] Therefore, zwitterionic carbamates of glycine are readily hydrolyzed to (bi)carbonate salts (Eq. 7), which results in high concentrations of (bi)carbonate compared to carbamate in glycine-doped sorbents. On the other hand, carbamates of piperazine (piperazine carbamate and piperazine dicarbamate) are relatively stable and remain as the dominant species (Eq. 6).[27,34] Carbamates have been found to be challenging to convert electrochemically either due to difficulty in liberating appreciable amount of CO_2 from the carbamate solution,[38–40] or due to the blockage of the active cathode surface by bulky ammonium cation (i.e., RNH_3^+).[13] Consistent with other studies, our data suggests that bicarbonate-enriched solutions are more readily converted into CO than carbamate-enriched solutions.[38,41,42]

Formation of an intermediate:

$$CO_{2(aq)} + R_1R_2NH(aq) \rightleftharpoons R_1R_2NH^+COO^-_{(aq)} \quad (4)$$

Deprotonation of the intermediate by a base:

$$R_1R_2NH^+COO^-_{(aq)} + B_{(aq)} \rightleftharpoons R_1R_2NCOO^-_{(aq)} + BH^+_{(aq)} \quad (5)$$

$$CO_{2(aq)} + 2R_1R_2NH_{(aq)} \rightleftharpoons R_1R_2NCOO^-_{(aq)} + RNH_3^+{}_{(aq)} \quad (6)$$

$$R_1R_2NCOO^-_{(aq)} + H_2O_{(l)} \rightleftharpoons R_1R_2NH_{(aq)} + HCO_3^-{}_{(aq)} \quad (7)$$

The CO_2 capture rates in the CCR increased by 2-fold as the glycine concentration was increased from 0 to 0.1 M (Fig. S5), but a 5% decrease in FE_{CO} was also observed (Fig. 3). This result is consistent with the FE_{CO} data collected during independent operation of the bicarbonate electrolyzer (Fig. S3), and can be attributed to the formation of carbamates in the K_2CO_3 solution. The CO_2 capture rate increased minimally (by a factor of 1.9 initially) as the glycine concentration was further increased to 0.5 M while the FE_{CO} decreased by another 7%. These results indicate that a low concentration of glycine can effectively catalyze (bi)carbonate formation in the CO_2 absorption column with minimal impact to the FE_{CO} of the electrolyzer.

The further scaling of the laboratory-scale CCR unit discussed in this work requires achieving both a high CO_2 capture rate and a high rate of electrolytic CO production. The former requires a higher pH and the latter requires a lower pH. To address this challenge, we introduced glycine to the solution to increase CO_2 capture rates at lower pH values. At the scale of our experimental apparatus, 0.1 M glycine in 1 M K_2CO_3 yielded the highest CO_2 capture rate without compromising syngas formation.

Conclusion

Here, we demonstrate that the OH^- produced from the electrochemical CO_2 reduction reaction in a bicarbonate electrolyzer can successfully regenerate the alkalinity of a reactive carbon solution to enable sustainable CO_2 capture for a prolonged period of time. We achieved this by building an integrated CO_2 capture and conversion device ("coupled carbon reactor") that uses 1 M K_2CO_3 as the capture media. The coupled carbon reactor (CCR) consists of a packed bed CO_2 absorption column, a bicarbonate electrolyzer, and a gas-liquid separator. The CCR reported in this work captures 0.27 g hr^{-1} of CO_2 and produces 0.077 g hr^{-1} of CO without any promoters. When 0.1 M glycine is added to 1 M K_2CO_3 as a capture promoter, the CO formation rate slightly decreases to 0.067 g hr^{-1}, but CO_2 capture rate increases to 0.35 g hr^{-1}. It is therefore imperative to balance the tradeoffs of CO_2 capture and CO_2 reduction to mediate integrated reactive carbon electrolysis. This work is the first demonstration of capturing CO_2 from simulated flue gas using a reactive carbon solution (e.g., (bi)carbonate-enriched solution) and subsequently converting the reactive carbon solution into syngas.

Experimental procedure

Materials

K_2CO_3 (ACS reagent, ≥99.0%, Sigma Aldrich, USA), KOH (ACS reagent, ≥85%, pellets, Sigma Aldrich, USA), ethylenediaminetetraacetic acid (EDTA; 99%, Sigma Aldrich, USA), silver nanoparticles (<100 nm particle size, contains PVP as dispersant, 99.5% trace metals basis, Sigma Aldrich, USA), glycine (ReagentPlus®, ≥99% (HPLC), Sigma Aldrich, USA), and piperazine (ReagentPlus®, 99%, Sigma Aldrich, USA) were purchased and used as received. Fumasep-FBM® bipolar membranes, Freudenberg H23 carbon papers, and Nafion® D2020 (20 wt% in a mixture of lower aliphatic alcohols and water) were purchased from Fuel Cell Store, USA. Nickel foam anodes were purchased from MTI Corporation, USA.

Materials preparation

Nickel foam anode was cut into 4 cm^2 and used as-received without any modification. Cathodes were prepared by spray-coating silver nanoparticles onto carbon papers. The cathode catalyst inks were prepared by mixing 27 mg of silver nanoparticles (<100 nm) with 10 μL of 20 wt% Nafion® (Nafion Dispersion D2020) in 9 mL of ethanol and the catalyst ink was sonicated for 20 min for even dispersion. Carbon papers were cut into 4 cm^2. The cathode catalyst inks were then deposited onto these carbon papers using an air-brush until the catalyst loading was 2 mg cm^{-2} (gravimetric measurement). The air pressure for the air-brush was set to 20 psi. The hotplate below the cathode samples was heated to 150°C to accelerate solvent evaporation during the spray-coating process. A bipolar membrane was cut in a larger area (3.5 × 3.5 cm^2) to accommodate sealing and was used as-is.

Electrolyzer design and assembly

Details of the bicarbonate electrolyzer design used in this work is reported in our previous works [1]. In brief, the bicarbonate electrolyzer consists of stainless steel housing plates and flow plates with

serpentine flow patterns that sandwich the membrane electrode assembly (MEA). The MEA consists of a nickel foam anode, a carbon paper cathode spray-coated with silver nanoparticles, and a bipolar membrane (BPM) separating the anode and cathode compartments. The BPM was configured in reverse-bias, meaning the cation exchange layer faces the cathode and the anion exchange layer faces the anode. The active area is 2 × 2 cm^2 which equates to a geometric surface area of 4 cm^2. This geometric surface area was used to calculate the current density reported in this work. The entire components of the assembly were pressed against each other with no gap ("zero-gap architecture"). The assembly was tightened with 6 bolts of 6.35 mm diameter to a torque of 4.5 N · m.

CO_2 absorber design

A lab-scale CO_2 absorber was designed in-house as a modular-based stainless steel column. The CO_2 absorber has two stages, each stage with different height and diameter. The bottom stage (height: 11.5 cm, inner diameter: 8 cm) serves as a reservoir for excess liquid sorbent. The top stage (height: 30 cm and inner diameter: 4 cm) is the packed column that encloses packing materials (Fig. S1). The top and bottom stages were separated by a piece of stainless steel mesh to hold packing materials in the packed column, but allow flow of liquid and gas between the reservoir and the packed column. The liquid sorbent exits the CO_2 absorber from the reservoir and enters the absorber from the top of the packed column through a liquid distributor. The liquid distributor was designed as a single-inlet and multi-outlet module (mimicking a shower head) to enhance the liquid wetting of the bed of packings. The gas enters into the CO_2 absorber in the overhead of the reservoir and exits at the gas outlet near the top of the packed column. Polypropylene Raschig rings (length: 0.8 cm; outer diameter: 0.6 cm; and inner diameter: 0.4 cm) were used as the packing materials. Raschig rings were randomly poured into the packed column ("random packing"). The packing height measured 20 cm.

Coupled carbon reactor experimental procedure

The coupled carbon reactor (CCR) consists of three main components; a CO_2 absorber; a bicarbonate electrolyzer; and a gas-liquid separator. The liquid outlet of the CO_2 absorber was connected to the liquid inlet of the bicarbonate electrolyzer. The liquid outlet of the bicarbonate electrolyzer was connected to the liquid inlet of the separator. Finally, the liquid outlet of the separator was connected to the liquid inlet of the CO_2 absorber. Two peristaltic pumps (43205K316, McMaster-Carr, USA) were installed to circulate the liquid sorbent; one between the outlet of the CO_2 absorber and the inlet of the bicarbonate electrolyzer and another one between the outlet of the separator and the inlet of the CO_2 absorber. Two peristaltic pumps were used to maintain the liquid level in the separator constant.

A liquid sorbent was first prepared by mixing 69 g of K_2CO_3 and 2.92 g of EDTA in 500 mL of deionized water (i.e., 1 M K_2CO_3 and 20 mM EDTA). A 20 mM EDTA was added to the 1 M K_2CO_3 to help prevent electrolyte impurities from electrodepositing on the electrode surface. For the studies involving CO_2 capture promoters (e.g., piperazine and glycine), the appropriate amounts of rate promoters were added to the liquid sorbent accordingly. A 1 M K_2CO_3 liquid sorbent was circulated at 100 mL min^{-1} for the duration of all experiments. A 175 sccm of N_2 continuously purged the headspace of the gas liquid separator to carry electrolysis products from the liquid sorbent to the gas chromatograph (GC; SRI-8610C, SRI Instruments, USA). A 1000 sccm of simulated flue gas entered the CO_2 absorber from the bottom and exited at the top of the CO_2 absorber. A gaseous mixture of 20% CO_2 and 80% N_2 was used as the simulated flue gas in this study. A 500 mL of 1 M KOH was circulated through the anode compartment at a flow rate of 40 mL min^{-1} using a peristaltic pump (9154K53, McMaster-Carr, USA).

Two-electrode electrolysis experiments were conducted at ambient pressure and temperature with a custom designed zero-cap electrolyzer using a power supply (2260B-30-72 720W, Keithley Instruments, USA). Current density is expressed as the total current applied divided by the geometric surface area of the electrodes (4 cm^2).

Product analysis

The composition of the gaseous products from the separator was analyzed with a GC at different time lengths. The GC was equipped with a packed MolSieve 5A column and a packed HaySep D column. Argon (Praxair, 99.999%) was used as the carrier gas. A flame ionization detector (FID) with a methanizer was used to quantify reduced carbon products (e.g., CO, CH_4, C_2H_4, C_2H_6, and C_3H_8) and CO_2. A thermal conductivity detector (TCD) was used to quantify H_2. The GC was calibrated by injecting different calibration gas mixes from NorLAB containing CO, CO_2, H_2, CH_4, C_2H_6, and C_3H_8 at concentrations ranging from 100-50000 ppm for each gas (balance N_2).

The Faradaic efficiency (FE) was calculated based on gas concentrations obtained from GC analyses using Faraday's law of electrolysis:

$$FE_i = \frac{x_i z_i \dot{n} F}{I} \quad \text{(S1)}$$

where z_i is the number of electrons transferred per mole of gaseous product i involved in the reduction reaction, F is Faraday's constant, x_i is the mole fraction of gaseous product i in the gaseous mixture analyzed using GC, $\dot{n}$ is the molar flow rate, and I is the total applied current. The molar flow rate was derived from the volumetric flow rate Q by the ideal gas law.

The *in situ* generated CO_2 was calculated assuming CO was the only reduced carbon product in this study:

$$i\text{-}CO_2 \text{ (ppm)} = [CO_2]_{\text{unreacted}} + [CO] \quad \text{(S2)}$$

where i-CO_2 is the concentration of *in situ* generated CO_2 and [CO] and $[CO_2]_{\text{unreacted}}$ represent the concentrations of CO and unreacted CO_2 measured by GC at the outlet of the electrolyzer.

The carbon efficiency was calculated by dividing the [CO] at the outlet by the total amount of CO_2 generated *in situ* (i-CO_2):

$$Carbon\ utilization\ (\%) = \frac{[CO]}{i{-}CO_2} \times 100\% \quad \text{(S3)}$$

Acknowledgements

The authors are grateful to the Canadian Natural Science and Engineering Research Council (RGPIN-2018-06748), Canadian Foundation for Innovation (229288), Canadian Institute for Advanced Research (BSE-BERL-162173), and the Canada Research Chairs, for financial support. This research was undertaken thanks, in part, to funding from the Max Planck-UBC-UTokyo Center for Quantum Materials and the Canada First Research Excellence Fund, Quantum Materials and Future Technologies Program.

Author contributions

Conceptualization: CPB, YK, EWL; Methodology: YK, EWL, CEBW; Investigation: YK, CD, GLS, AV; Visualization: YK, EWL; Funding acquisition: CPB; Supervision: CPB; Writing – original draft: CPB, YK, EWL; Writing – review & editing: All authors

Competing interests

Authors C.P.B., E.W.L. have filed patent applications for the technology used in this work (PCT International Application No. PCT/CA2019/050539, Filed April 2019; Filed and pending in US (Serial # 17/050,319), Canada (Serial # 3,098,176), and Europe (Serial # 19791477.3)).

Supplementary Material

Materials and methods; Supplementary notes 1 to 3; Figs. S1 to S7; Tables S1 and S2.

References

1. Keith, D.W., Holmes, G., St. Angelo, D., and Heidel, K. (08/2018). A Process for Capturing CO_2 from the Atmosphere. Joule *2*, 1573–1594.

2. Roussanaly, S., Rubin, E., Der Spek, M., Booras, G., Berghout, N., Fout, T., Garcia, M., Gardarsdottir, S., Kuncheekanna, V., Matuszewski, M., et al. (2021). Towards improved guidelines for cost evaluation of carbon capture and storage (National Energy Technology Laboratory - In-house Research) 10.2172/1779820.

3. Barecka, M.H., Ager, J.W., and Lapkin, A.A. (2021). Carbon neutral manufacturing via on-site CO_2 recycling. iScience *24*, 102514.

4. Barecka, M.H., Ager, J.W., and Lapkin, A.A. (2021). Techno-economic assessment of emerging CO_2 electrolysis technologies. STAR Protoc *2*, 100889.

5. Li, T., Lees, E.W., Goldman, M., Salvatore, D.A., Weekes, D.M., and Berlinguette, C.P. (06/2019). Electrolytic Conversion of Bicarbonate into CO in a Flow Cell. Joule *3*, 1487–1497.

6. Lees, E.W., Goldman, M., Fink, A.G., Dvorak, D.J., Salvatore, D.A., Zhang, Z., Loo, N.W.X., and Berlinguette, C.P. (2020). Electrodes Designed for Converting Bicarbonate into CO. ACS Energy Lett. *5*, 2165–2173.

7. Zhang, Z., Lees, E.W., Habibzadeh, F., Salvatore, D.A., Ren, S., Simpson, G.L., Wheeler, D.G., Liu, A., and Berlinguette, C.P. (2022). Porous metal electrodes enable efficient electrolysis of carbon capture solutions. Energy Environ. Sci. *Advance Article*. 10.1039/D1EE02608A.

8. Zhang, Z., Lees, E.W., Ren, S., Mowbray, B.A.W., Huang, A., and Berlinguette, C.P. (2022). Conversion of Reactive Carbon Solutions into CO at Low Voltage and High Carbon Efficiency. ACS Cent Sci *8*, 749–755.

9. Ozden, A., García de Arquer, F.P., Huang, J.E., Wicks, J., Sisler, J., Miao, R.K., O'Brien, C.P., Lee, G., Wang, X., Ip, A.H., et al. (2022). Carbon-efficient carbon dioxide electrolysers. Nat Sustain, 1–11.

10. Gutiérrez-Sánchez, O., Bohlen, B., Daems, N., Bulut, M., Pant, D., and Breugelmans, T. (2022). A state‐of‐the‐art update on integrated CO_2 capture and electrochemical conversion systems. ChemElectroChem *9*. 10.1002/celc.202101540.

11. Xiao, Y.C., Gabardo, C.M., Liu, S., Lee, G., Zhao, Y., O'Brien, C.P., Miao, R.K., Xu, Y., Edwards, J.P., Fan, M., et al. (2023). Direct carbonate electrolysis into pure syngas. EES. Catal. *1*, 54–61.

12. Diaz, L.A., Gao, N., Adhikari, B., Lister, T.E., Dufek, E.J., and Wilson, A.D. (2018). Electrochemical production of syngas from CO_2 captured in switchable polarity solvents. Green Chem. *20*, 620–626.

13. Lee, G., Li, Y.C., Kim, J.-Y., Peng, T., Nam, D.-H., Sedighian Rasouli, A., Li, F., Luo, M., Ip, A.H., Joo, Y.-C., et al. (2021). Electrochemical upgrade of CO_2 from amine capture solution. Nat Energy *6*, 46–53.

14. Li, Y.C., Lee, G., Yuan, T., Wang, Y., Nam, D.-H., Wang, Z., García de Arquer, F.P., Lum, Y., Dinh, C.-T., Voznyy, O., et al. (2019). CO_2 Electroreduction from Carbonate Electrolyte. ACS Energy Lett. *4*, 1427–1431.

15. Lee, J., Liu, H., and Li, W. (2022). Bicarbonate Electroreduction to Multicarbon Products Enabled by Cu/Ag Bilayer Electrodes and Tailored Microenviroments. ChemSusChem *15*, e202201329.

16. Gao, N., Quiroz-Arita, C., Diaz, L.A., and Lister, T.E. (2021). Intensified co-electrolysis process for syngas production from captured CO2. Journal of CO2 Utilization *43*, 101365.

17. Larrea, C., Torres, D., Avilés-Moreno, J.R., and Ocón, P. (2022). Multi-parameter study of CO_2 electrochemical reduction from concentrated bicarbonate feed. Journal of CO2 Utilization *57*, 101878.

18. Schaidle, J. (2022). Reactive Carbon Capture: Status, Challenges, and Opportunities.

19. Benson, H.E., Field, J.H., and Jimeson, R.M. (1954). Carbon dioxide absorption employing hot potassium carbonate solutions. Chem. Eng. Prog. *50*, 356–364.

20. Kannangara, M., Shadbahr, J., Vasudev, M., Yang, J., Zhang, L., Bensebaa, F., Lees, E., Simpson, G., Berlinguette, C., Cai, J., et al. (2022). A standardized methodology for economic and carbon footprint assessment of CO_2 to transport fuels: Comparison of novel bicarbonate electrolysis with competing pathways. Appl. Energy *325*, 119897.

21. Wappel, D., Joswig, S., Khan, A.A., Smith, K.H., Kentish, S.E., Shallcross, D.C., and Stevens, G.W. (2011). The solubility of sulfur dioxide and carbon dioxide in an aqueous solution of potassium carbonate. Int. J. Greenhouse Gas Control *5*, 1454–1459.

22. Smith, K., Xiao, G., Mumford, K., Gouw, J., Indrawan, I., Thanumurthy, N., Quyn, D., Cuthbertson, R., Rayer, A., Nicholas, N., et al. (2014). Demonstration of a Concentrated Potassium Carbonate Process for CO_2 Capture. Energy Fuels *28*, 299–306.

23. Borhani, T.N.G., Azarpour, A., Akbari, V., Wan Alwi, S.R., and Manan, Z.A. (2015). CO_2 capture with potassium carbonate solutions: A state-of-the-art review. Int. J. Greenhouse Gas Control *41*, 142–162.

24. Anderson, C., Harkin, T., Ho, M., Mumford, K., Qader, A., Stevens, G., and Hooper, B. (2013). Developments in the CO2CRC UNO MK 3 Process: A Multi-component Solvent Process for Large Scale CO_2 Capture. Energy Procedia *37*, 225–232.

25. Zhang, Z., Melo, L., Jansonius, R.P., Habibzadeh, F., Grant, E.R., and Berlinguette, C.P. (2020). pH Matters When Reducing CO_2 in an Electrochemical Flow Cell. ACS Energy Lett. *5*, 3101–3107.

26. Angulo, A., van der Linde, P., Gardeniers, H., Modestino, M., and Fernández Rivas, D. (2020). Influence of Bubbles on the Energy Conversion Efficiency of Electrochemical Reactors. Joule *4*, 555–579.

27. Cullinane, J.T., and Rochelle, G.T. (2004). Carbon dioxide absorption with aqueous potassium carbonate promoted by piperazine. Chem. Eng. Sci. *59*, 3619–3630.

28. Thee, H., Nicholas, N.J., Smith, K.H., da Silva, G., Kentish, S.E., and Stevens, G.W. (2014). A kinetic study of CO_2 capture with potassium carbonate solutions promoted with various amino acids: Glycine, sarcosine and proline. Int. J. Greenhouse Gas Control *20*, 212–222.

29. Hu, G., Smith, K.H., Wu, Y., Kentish, S.E., and Stevens, G.W. (2017). Screening Amino Acid Salts as Rate Promoters in Potassium Carbonate Solvent for Carbon Dioxide Absorption. Energy Fuels *31*, 4280–4286.

30. Caplow, M. (1968). Kinetics of carbamate formation and breakdown. J. Am. Chem. Soc. *90*, 6795–6803.

31. Danckwerts, P.V. (1979). The reaction of CO_2 with ethanolamines. Chem. Eng. Sci. *34*, 443–446.

32. Blauwhoff, P.M.M., Versteeg, G.F., and Van Swaaij, W.P.M. (1984). A study on the reaction between CO_2 and alkanolamines in aqueous solutions. Chem. Eng. Sci. *39*, 207–225.

33. Versteeg, G.F., and van Swaaij, W.P.M. (1988). On the kinetics between CO_2 and alkanolamines both in aqueous and non-aqueous solutions—I. Primary and secondary amines. Chem. Eng. Sci. *43*, 573–585.

34. Lim, J.-A., Kim, D.H., Yoon, Y., Jeong, S.K., Park, K.T., and Nam, S.C. (2012). Absorption of CO_2 into Aqueous Potassium Salt Solutions of l-Alanine and l-Proline. Energy Fuels *26*, 3910–3918.

35. Hu, G., Nicholas, N.J., Smith, K.H., Mumford, K.A., Kentish, S.E., and Stevens, G.W. (2016). Carbon dioxide absorption into promoted potassium carbonate solutions: A review. Int. J. Greenhouse Gas Control *53*, 28–40.

36. Kumar, P.S., Hogendoorn, J.A., Versteeg, G.F., and Feron, P.H.M. (2003). Kinetics of the reaction of CO_2 with aqueous potassium salt of taurine and glycine. AIChE J. *49*, 203–213.

37. Guo, D., Thee, H., Tan, C.Y., Chen, J., Fei, W., Kentish, S., Stevens, G.W., and da Silva, G. (2013). Amino Acids as Carbon Capture Solvents: Chemical Kinetics and Mechanism of the Glycine + CO_2 Reaction. Energy Fuels *27*, 3898–3904.

38. Chen, L., Li, F., Zhang, Y., Bentley, C.L., Horne, M., Bond, A.M., and Zhang, J. (2017). Electrochemical Reduction of Carbon Dioxide in a Monoethanolamine Capture Medium. ChemSusChem *10*, 4109–4118.

39. Pérez-Gallent, E., Vankani, C., Sánchez-Martínez, C., Anastasopol, A., and Goetheer, E. (2021). Integrating CO_2 Capture with Electrochemical Conversion Using Amine-Based Capture Solvents as Electrolytes. Ind. Eng. Chem. Res. *60*, 4269–4278.

40. Ahmad, N., Chen, Y., Wang, X., Sun, P., Bao, Y., and Xu, X. (2022). Highly efficient electrochemical upgrade of CO_2 to CO using AMP capture solution as electrolyte. Renewable Energy *189*, 444–453.

41. Jerng, S.E., and Gallant, B.M. (2022). Electrochemical reduction of CO_2 in the captured state using aqueous or nonaqueous amines. iScience *25*, 104558.

42. Kim, J.H., Jang, H., Bak, G., Choi, W., Yun, H., Lee, E., Kim, D., Kim, J., Lee, S.Y., and Hwang, Y.J. (2022). The insensitive cation effect on a single atom Ni catalyst allows selective electrochemical conversion of captured CO_2 in universal media. Energy Environ. Sci. *15*, 4301–431